Table X. Electron Correlation Effects on the Si-Si Bond Distance and Stretching Force Constant in the Si_2H_4 System

	R_{SiSi} (Å)		K_{SiSi} (mdyn/Å)	
	SCF	CEPA	SCF	CEPA
disilene				
^1Ag	2.127	2.171	3.50	2.28
^3B	2.407	2.378	1.53	1.51
silylsilylene				
$^1A'$	2.479	2.453	1.30	1.24
$^3A''$	2.395	2.374	1.57	1.51

in Table X. As expected, in singlet disilene the bond distance is increased and the force constant is decreased by inclusion of electron correlation effects. In the other cases, in which Si–Si single bonds are involved, a reduction of the SiSi bond distance is observed. In the pair-energy approach one can visualize the situation in the following way: for singlet disilene the intrapair contributions of the Si–Si σ and π bonds increase in absolute value upon stretching the SiSi bond. This leads to the well-known increase of the equilibrium bond distance when compared to the SCF value. For the single bonded systems the just-mentioned effect is not so important. An additional, opposing factor becomes relevant, namely, the decrease (in absolute value) of interpair energies which leads to a reduction of the equilibrium distance. A similar, but not so pronounced effect can be found in the carbon-containing systems as well (see Figurs 1 and 2).

4. Summary

Geometries, harmonic force fields, and stability differences have been derived in a systematic and consistent way for the title molecules. One question of great chemical interest is the double-bond character of the SiSi bond in disilene. We do not attempt to give an elaborate discussion on that problem but simply want to look at a few properties of the energy surface and make a comparison with the corresponding quantities for ethylene and silaethylene.

The SiSi bond length in singlet disilene is considerably shorter than that in purely single-bonded compounds like silylsilylene. The effects are comparable with those for C_2H_4 and SiH_2CH_2. The SiSi force constant in disilene is larger than in silylsilylene. These two factors demonstrate the double-bond character of the SiSi bond in disilene. On the other hand, disilene is not so rigid as ethylene or silaethylene. In fact, it has been shown in ref 8 and 17 that the equilibrium structure of disilene is not completely planar or at least that the potential curve for the out-of-plane motion of the SiH_2 groups is very flat in the region of the energy minimum.

From a practical point of view it is interesting to note that the geometries obtained from basis sets including d functions (especially on silicon) do not deviate substantially from those calculated without d functions. However, these findings should be considered with caution. There is, of course, no guarantee that for other, even similar systems the same situation will hold.

Acknowledgment. This work was carried out under the auspices of the WTZ-treaty between Austria and the German Democratic Republic. We thank Professor H. F. Schaefer III and his coworkers for a CDC version of their Hartree–Fock and gradient program. Generous computer time at the CDC CYBER 170 computers of the IEZ Vienna is gratefully acknowledged.

Registry No. Si_2H_4, 15435-77-5; SiH_3SiH, 50420-90-1; SiH_2CH_2, 51067-84-6; SiH_3CH, 66605-30-9; CH_3SiH_2, 24669-75-8; $H_2C{=}CH_2$, 74-85-1; CH_3CH, 4218-50-2.

Electronic Structure of Long Polyiodide Chains

Miklős Kertész* and Ferenc Vonderviszt

Contribution from the Central Research Institute for Chemistry, Hungarian Academy of Sciences, H-1525 Budapest, Hungary. *Received February 1, 1982*

Abstract: The electronic structure of periodic one-dimensional polyiodides is studied for both $(I_3^-)_\infty$ and $(I_5^-)_\infty$ systems. The deformation from the equidistant arrangement toward the $(I_3^-)_\infty$ structure, as well as from the linear toward zigzag chains, permits a rationalization of the experimentally found structures. The role of electron delocalization in their compounds with high electrical conductivity is examined.

Short contacts of the I_3^- or I_5^- polyiodide ions aggregated together in several complex materials of channel inclusion compounds[1-22] indicate electron delocalization[8,15,19-21] along these long polyiodide (PI) chains. The crystal structure data of these materials indicate different degrees of delocalization. It has been repeatedly suggested[5,8,15,19,21] that electronic conduction may take

---

(1) (a) R. E. Rundle, J. F. Foster, and R. R. Baldwin, *J. Am. Chem. Soc.*, **66**, 2116 (1944); (b) C. D. West, *J. Chem. Phys.*, **15**, 689 (1947).

(2) (a) G. C. Pimentel, *J. Chem. Phys.*, **19**, 446 (1951); (b) R. J. Hach and R. E. Rundle, *J. Am. Chem. Soc.*, **73**, 4321 (1951).

(3) F. Cramer, *Recl. Trav. Chim. Pays-Bas* **75**, 891 (1956).

(4) J. M. Reddy, K. Knox, and M. B. *Robin*, *J. Chem. Phys.*, **40**, 1082 (1964).

(5) (a) K. Huml, *Acta Crystallogr.*, **22**, 29 (1967); (b) V. Hadek, *J. Chem. Phys.*, **49**, 5202 (1968); (c) V. Hadek, P. Zach, K. Ulbert, and J. Honzl, *Collect. Czech. Chem. Commun.*, **34**, 3139 (1969).

(6) A. Gleizes, T. J. Marks, and J. A. Ibers, *J. Am. Chem. Soc.*, **97**, 3545 (1975).

(7) H. Endres, H. J. Keller, M. H.-Belombe, W. Moroni, H. Pritzkow, and J. Weiss, *Acta Crystallogr., Sect. A*, **32**, 954 (1976).

(8) (a) J. Kommandeur and F. R. Hall, *J. Chem. Phys.*, **34**, 129 (1961); (b) R. Bersohn and C. Isenberg, *ibid.*, **35**, 1640 (1961).

(9) a) L. I. Buravov, G. I. Zvereva, V. F. Kaminskii, C. P. Rosenberg, M. L. Khidekel, R. P. Shibaeva, and I. F. Shchegolev, *J. Chem. Soc., Chem. Commun.*, 720 (1976); (b) D. L. Smith and H. R. Luss, *Acta Crystallogr., Sect. B*, **33**, 1744 (1977); (c) R. B. Samoano, S. P. S. Yen, V. Hadek, S. K. Khanna, M. Novotny, T. Datta, A. M. Hermann, and J. A. Woollam, *Phys. Rev. B*, **17**, 2853 (1978).

(10) H. V. Düker, B. Freckmann, H. Niebuhr, M. Plewa, and K. F. Tebbe, *Z. Kristallogr., Kristallgeom., Kristallphys., Kristallchem.* **149**, 120 (1979).

(11) (a) B. Hilti and C. W. Mayer, *Helv. Chim. Acta*, **61**, 501 (1978); (b) G. Rihs, Ciba-Geigy Internal Communication 1978.

(12) (a) H. Strzelecka, C. Weyl, and J. Rivory, *Lect. Notes Phys.* **96**, 348 (1979); (b) S. Flandrois, C. Coulon, J. Amiell, P. Delhaes, and P. Dupnis, *ibid.*, **96**, 188 (1979); (c) D. Chasseau, A. Filhol, J. Gautier, C. Hauw, and W. Steiger, *Chem. Scr.*, **17**, 97 (1981).

(13) (a) F. H. Herbstein and M. Kapon, *Nature (London), Phys. Sci.*, **239**, 153 (1972). (b) J. A. Kramer, F. H. Herbstein, and D. N. Hendrickson, *J. Am. Chem. Soc.*, **102**, 2293 (1980).

(14) F. H. Herbstein and M. Kapon, *Acta Crystallogr., Sect. A*, **28**, S74 (1972).

(15) M. Noltenmeyer and W. Saenger, *Nature (London)*, **259**, 629 (1976).

(16) F. Cramer, U. Bergmann, P. C. Manor, M. Noltenmayer, and W. Saenger, *Justus Liebigs Ann. Chem.*, 1169 (1976).

(17) (a) M. Noltenmeyer and W. Saenger, *J. Am. Chem. Soc.*, **102**, 2710 (1980); (b) R. C. Teitelbaum, S. L. Reeby, and T. J. Marks, *ibid.*, **102**, 3322 (1980).

(18) H. Endres and J. P. Pouget, *Chem. Scr.*, **17**, 137 (1981).

(19) J. H. Perlstein, *Angew. Chem.*, **89**, 534 (1977).

(20) M. M. Labes, *Mol. Cryst. Liq. Cryst.*, **32**, 161 (1976).

0002-7863/82/1504-5889$01.25/0

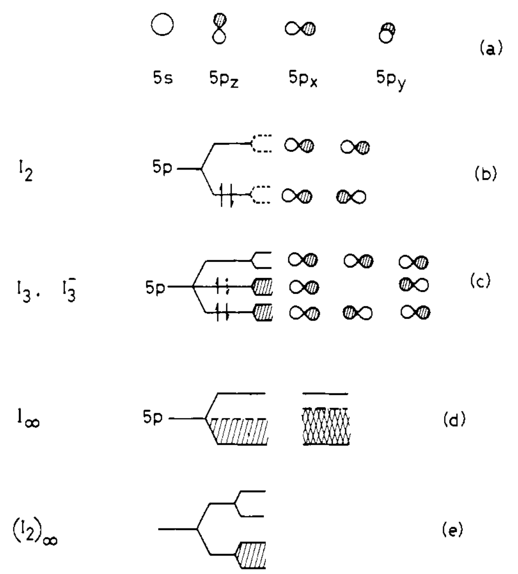

Figure 1. Schematic valence orbital diagrams in iodides: (a) Iodine atom, (b) I_2 molecule, (c) I_3 molecule and I_3^- ion (dotted) (the two occupied and one empty energy bands correspond to $(I_3^-)_\infty$ chains), (d) half-filled band of the $(I)_\infty$ and two-thirds filled band of the $(I_3^-)_\infty$ equidistant chains, (e) a filled and an empty band of the $(I_2)_\infty$ chain. The shaded area indicates the double occupancy of each band orbital in the shaded region.

place along the polyiodide chains at least in some of these materials, as, e.g., the $12I\cdot5(C_6H_5NHC_6H_4NHC_6H_5)$ complex[19] as well as the $(\text{benzophenone})_9(KI)_2I_7CHCl_3$ canal complex.[21] In some of the other well-conducting complexes with PI chains such as TTT_2I_3,[9] electrical conduction may also take place along the chains of stacking donors. In others[22] the I–I contacts are too large for any delocalization along the PI's, and only the stacking interaction of donors permits high conductivity.

Polyiodides occur in a wide variety of crystals and structures. The basic structural units might be symbolically denoted by I^-, I_2, and I_3^-. The relatively strong interactions between these units lead to the formation of larger aggregates such as linear and zigzag chains and sheets which form in many cases ordered extended systems. The aim of this work is to rationalize the geometrical structures of PI chains found in X-ray experiments. We also comment on the degree of electron delocalization in these systems.

Crystal Orbitals

Infinite periodic models of various $(I_3{}^q)_\infty$ and $(I_5{}^q)_\infty$ chains have been investigated by the use of the energy band version[23] of the extended Hückel theory (EHT).[24] This non-self-consistent model permitted the easy comparison of a large number of structures with charge-transfer values q deviating from the idealized −1 value. The following parameters of iodine have been used. The valence-state ionization potentials were −18.0 eV (5s) and −12.7 eV (5p) with Slater exponents of 2.679 and 2.322, respectively.[25] Two neighbors were included in the lattice sum, and the k-space integrals were represented by five points. The computer program employed in the present work was originally written by Whangbo.[23c]

The σ-bonding in I_2 and I_3^-[26] is visualized in Figures 1b and 1c. The formation of an equidistant chain splits the levels[19] as illustrated in Figure 1d. A pairing distortion in the $(I)_\infty$ chain would split the band into an occupied and an empty band as shown in Figure 1e. The half-filled band of the equidistant $(I)_\infty$ is in principle metallic (owing to the presence of a half-filled band; see Figure 1d), and the band structures of $(I_3^-)_\infty$ and $(I_2)_\infty$ illustrated in Figures 1c and 1e, respectively, are nonmetallic. $(I_3^-)_\infty$, when equidistant, would have a metallic (two-thirds filled) band too, as the doubly dashed area in Figure 1d indicates. Other bands derived from lower lying σ- or π-type lone pairs are not illustrated in Figure 1. The 5s orbitals of iodine are not illustrated in Figure 1 for convienience, although they do mix in.

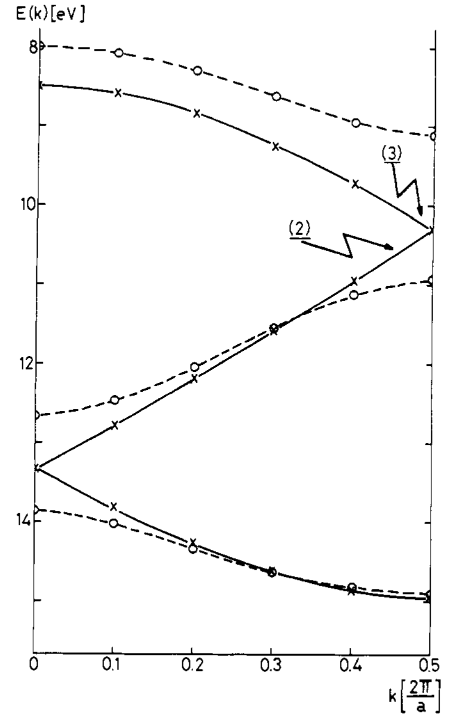

Figure 2. Energy band structure of the highest bands of the equidistant (—) and alternating (- - -) (δ = 0.15 Å) $(I_3^-)_\infty$ chain. Energetically the alternating structure is favored because level **2** is occupied and **3** is empty.

Equidistant and Distorted Linear Triiodide Chains

It is a well-known fact that the geometric structure of strictly one-dimensional (1-D) metallic systems is unstable[27] with respect to distortions leading to a new band structure with nonzero forbidden energy gap (Peierls theorem). This is also the case for the equidistant $(I_3^-)_\infty$ studied here. In Figure 2, we depict the band structure of the highest σ bands for both the equidistant and the distorted system with δ = 0.15 Å. The distortion parameter δ leading from the equidistant to the distorted $(I_3^-)_\infty$ structure is

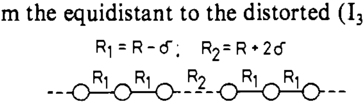

1

defined in **1**. In this scheme the distortion is energetically favorable, because only two of the three split bands ($\delta \neq 0$) are filled, leading to an energy gain in the $k = \pi/a$ ($a = 3R$) region of the Brillouin zone. In orbital language, the orbital **2** corresponding

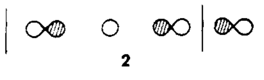

2

to the highest occupied level at $k = \pi/a$ becomes more bonding because of distortion **1**, at least in the vicinity of the equidistant structure. Similarly, destabilization results for the lowest empty orbital **3**.

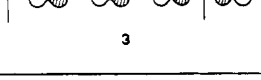

3

---

[21] M. M. Labes, M. Jones, H. I. Kao, L. Nichols, C. Hsu, and T. O. Poehler, *Mol. Cryst. Liq. Cryst.*, **52**, 419 (1979).

[22] (a) G. B. Johnson and C. R. Watson, *J. Chem. Phys.*, **64**, 2271 (1976); (b) B. A. Scott, S. J. LaPlaca, J. B. Torrance, B. D. Silverman, and B. Welber, *J. Am. Chem. Soc.*, **99**, 6631 (1977); (c) B. Hilti, C. W. Mayer, and G. Rihs, *Helv. Chim. Acta*, **61**, 1462 (1978).

[23] (a) A. Imamura, *J. Chem. Phys.*, **52**, 3168 (1970); (b) K. Morokuma, *Chem. Phys. Lett.*, **6**, 186 (1970); (c) M.-H. Whangbo, R. Hoffmann, and R. B. Woodward, *Proc. R. Soc. London, Ser. A*, **366**, 23 (1979).

[24] R. Hoffmann, *J. Chem. Phys.*, **39**, 1397 (1963).

[25] M.-H. Whangbo and M. J. Foshee, *Inorg. Chem.*, **20**, 113 (1980).

[26] (a) E. H. Wiebenga and D. Kracht, *Inorg. Chem.*, **8**, 733 (1969); (b) W. Gabes and M. A. M. Nijman-Meester, *ibid.*, **12**, 589 (1973).

[27] R. Peierls, "Quantum Theory of Solids", Oxford, 1955.

Table I. Experimentally Found Average I-I Distances, R, and δ Alternation Values as Defined in 1 for Several $(I_3^-)_\infty$ Chains

R, Å	δ, Å	cation, X	composition	remarks
3.10		starch		ref 1[a]
3.06	0	cyclodextrine		ref 3[a]
3.20	0.30	$C_6H_5CONH_2$	HI_3X_2	ref 4
3.14	0.15	*N,N'*-diphenyl-*p*-phenylenediamine	$I_{12}X_5$	ref 5a
3.271		(diphenylglyoximate)$_2$nickel	IX	disordered, ref 6
3.15	0.35	bis(1,2-benzoquinonedioximato)$_2$nickel	IX_2	disordered, ref 7
3.18	0.20	bis(tetrathiotetracene)	$I_{3+x}X_2$	($0 \leq x \leq 0.12$), ref 9, 11
2.95	0.21	$Cd(NH_3)_4$	I_6X	ref 10
2.98	0.20	Cu(ethylenediamine)$_2$	I_6X	ref 10
2.99	0.18	Ni(ethylenediamine)$_2$	I_6X	ref 10
3.23	0.23	tetramethylhexamethylenediammonium $TCNQ_2$[b]	I_2X	ref 12b
3.20	0.27	diphenylphenazinium	$I_{1.6}X$	ref 12c
3.22	0.23	trimethylammonium TCNQ	IX	ref 12c
3.22	0.27	isopentyldimethylammonium TCNQ	IX	ref 12c
3.28	0.34	methyl ethyl phenazinium	I_3X_2	ref 12c
3.23	0.26	$C_{16}H_{18}N_2$	$I_{1.6}X$	disordered, ref 18
		$C_{26}H_{22}N_2$	$I_{1.6}X$	

[a] Later work proved[16,17a] that these data probably correspond to disordered structures. [b] TCNQ: tetracyanoquinodimethane.

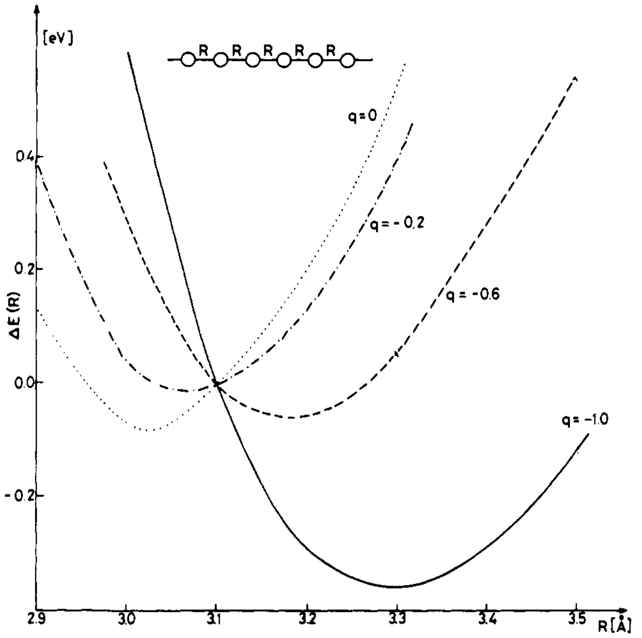

Figure 3. Relative total energy of equidistant $(I_3^q)_\infty$ chains at different charge-transfer values, q, as a function of the I–I distance, R. The curves are shifted together at an arbitrary point.

The total energy per elementary cell as a function of R for the equidistant chain is given in Figure 3. The most stable geometry is found at $R_{opt} = 3.3$ Å for $q = -1$. The effect of the distortion from the equidistant geometry can be seen from Figure 4, the optimal δ value being 0.15 Å for $q = -1$. All the these calculations were also performed with different values of the charge transfer (CT) parameter q. In order to compare the optimal geometry with experiment, we collected experimental R and δ values for several polytriiodide chains in Table I. The observed R values scatter in the range 2.95 to 3.28 Å, our theoretical value being close to the largest ones. The alternation parameters δ vary between 0.15 and 0.34 Å, our theoretical value being close to the lowest ones although a best experimental value would be closer to 0.3 Å.[32] This can be considered a reasonable agreement between theory and experiment in view of the simplicity of the theory and the variations of the experimental data. The latter are probably due partly to the differences in the Madelung potentials within one crystal[28] or among different hosts with slightly different periodicities. The calculated forbidden energy gap, E_{gap}, changes almost linearly with δ (Figure 5) in accord with the perturbation argument already mentioned for **2** and **3**. (For comparison with experiment, see the last section.)

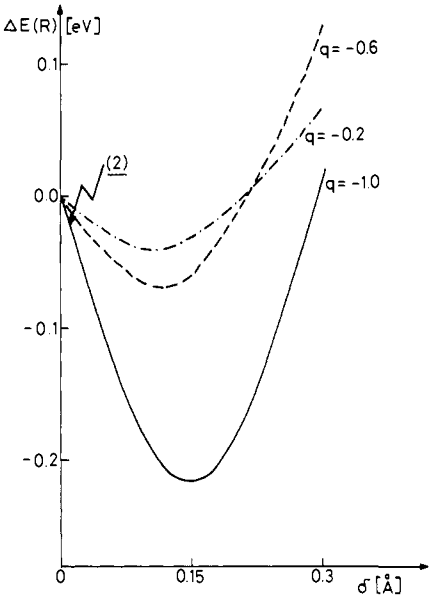

Figure 4. Relative total energy of alternating $(I_3^q)_\infty$ chains at different charge-transfer values, q, as a function of the alternations δ defined in **1**. R is fixed at 3.2 Å.

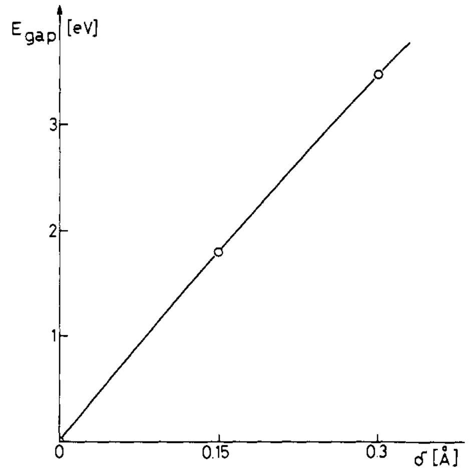

Figure 5. Energy gap in alternating $(I_3^-)_\infty$ chains as function of the distortion δ.

As the CT parameter varies from −1 to 0, the predicted optimal bond length of the equidistant chain decreases owing to a smaller occupation of the slightly antibonding-type highest occupied orbital **2** which is similar to the HOMO of the I_3^- ion as given in Figure 1c. The slight shift of the optimal value of δ as q changes (Figure

---

(28) K. Kamarâs and M. Kertêsz, *Solid-State Commun.*, **28**, 607 (1978).

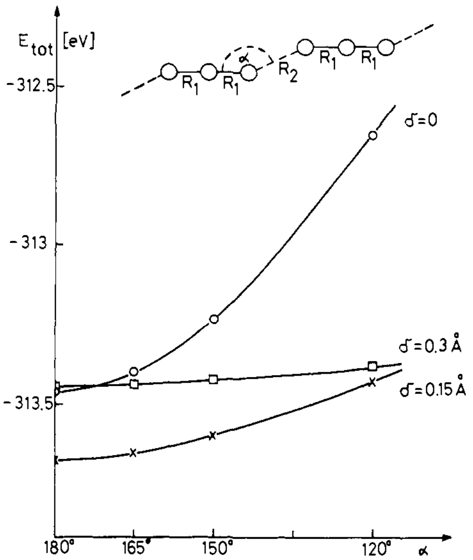

Figure 6. Total energy of zigzag chains at different distortions, δ, as a function of α (for definition, see inset). R is fixed at 3.2 Å.

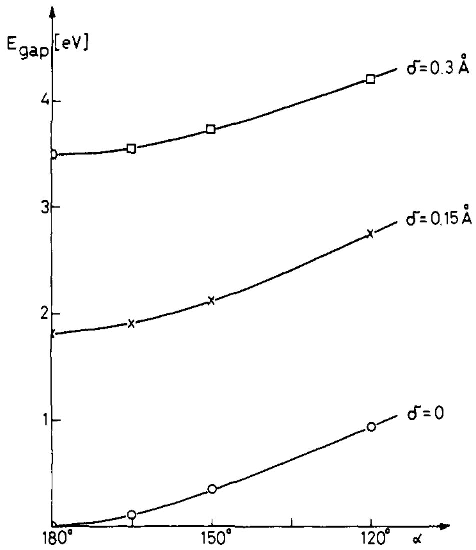

Figure 7. Energy gap of zigzag $(I_3^-)_\infty$ chains at different distortions, δ, as a function of α (for definition, see inset of Figure 6). R is fixed at 3.2 Å.

4) can be understood by recalling the slight antibonding character of this orbital which becomes depopulated in going from $q = -1$ to a smaller degree of CT. The rigidity of the geometrical parameters for small (~10%) deviation of q from -1 is a remarkable result explaining why stoichiometric and nonstoichiometric PI chains possess so similar geometries.

Zigzag $(I_3^-)_\infty$ Chains

Nonlinear structures are less stable than the linear ones for $(I_3^-)_\infty$ as can be seen from Figure 6, in full agreement with the fact that all observed structures are almost linear. This is due to the repulsion of the π lone pairs. This effect is less pronounced for the most alternating structure ($\delta = 0.3$ Å) simply because of the larger distance of the I_3^- units in it. The fact that nothing dramatic happens with the frontier orbitals upon bending the chain can be seen from the energy gap depicted as function of the zigzag angle α on Figure 7. The small energy needed to distort $(I_3^-)_\infty$ chains from the ideal $\alpha = 180°$ may allow the formation of zigzag chains in suitable hosts, which have not been observed yet, however.

$(I_5^-)_\infty$ Chains

The number of structurally well-characterized materials with $(I_5^-)_\infty$ chains is considerably less than those for the $(I_3^-)_\infty$ chains. Most of the reported structures in different hosts[13-17] exhibit disorder. Some of them have a zigzag shape[13] while others are nearly linear.[14-17] Some are close to the idealized $(I_2 - I^- - I_2)_\infty$ structure, while others resemble the $(I_3^- - I_2)_\infty$ structure. It is also known from the resonance Raman and I^{129} Mössbauer work of Teitelbaum et al.[17b] that in the amylose-iodine complex the $(I_5^-)_\infty$ form is favored over the $(I_3^- - I_2)_\infty$ form. A limited geometry optimization has been performed (Figure 8) on the basis of the idealized geometry which the polyiodide assumes in the trimesic acid as host.[14] The average bond length R within the I_5^- unit and the weakest interionic contact were kept constant. The parameter ϵ continuously carries the geometry from the $(I_5^-)_\infty$ model to the $(I_2 - I^- - I_2)_\infty$ model. $\epsilon = 0$ corresponds to equal I–I distances within the elementary cell, while $\epsilon = 0.5$ Å corresponds to the $(I_2 - I^- - I_2)_\infty$ limit. The distortion at $\epsilon = 0$ toward $\epsilon > 0$ values follows from the stabilization of the occupied orbital given in the inset of Figure 8. The predicted optimal ϵ values are definitely larger than the experimental value of 0.26 Å.[14] The change toward nonlinear (zigzag) structures is also possible as shown in Figure 9. In this case, however, other than linear structures have been

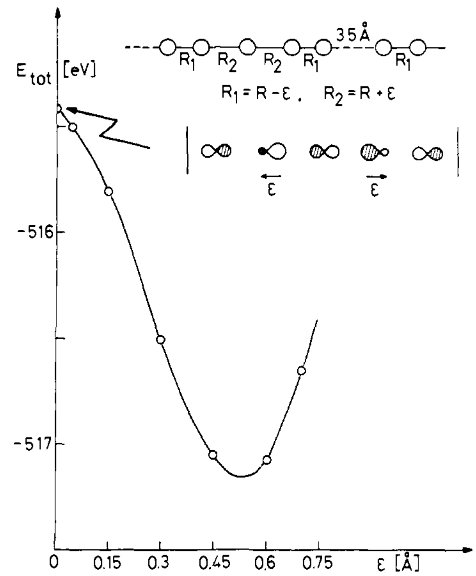

Figure 8. Total energy of linear $(I_5^-)_\infty$ chains as a function of the distortion, ϵ, as defined in the inset. The energy gain around $\epsilon = 0$ is due to the change of orbital interactioon illustrated in the inset. The structure in ref 14 corresponds to $\epsilon = 0.26$ Å.

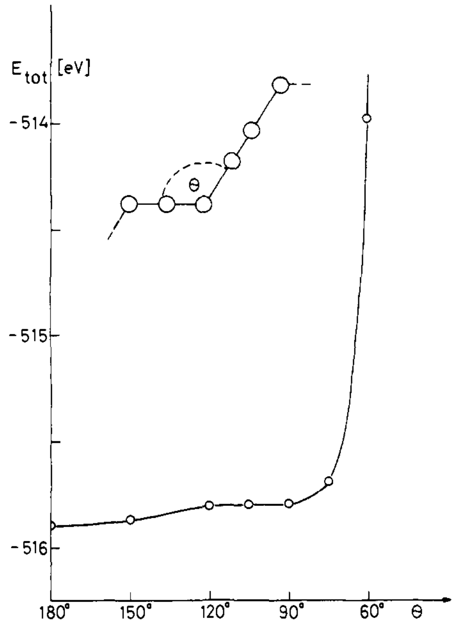

Figure 9. Total energy of zigzag $(I_3^- - I_2)_\infty$ chains as function of the deformation angle, θ, as defined in the inset. Bond lengths are taken from the experimental structure of Herbstein and Kapon.[13]

Table II. Calculated Effective Masses, m^*, and Deformation Potentials, $\delta\epsilon$, for Periodic $(I_3^-)_\infty$ and $(CH)_x$ Chains

	m^*/m_{el}		$\delta\epsilon$, eV	
	electron	hole	electron	hole
$(I_3^-)_\infty$	0.10	0.09	37.4	24.7
$(CH)_x$	0.10	0.11	4.6	3.4

observed[13] within the permissible range ($\theta > 80°$) depending on the shape of the inclusion channel for the PI's. The large increase of the energy below $\theta \simeq 80°$ is due to the strong antibonding character of the orbital **4** associated with π lone pairs.

4

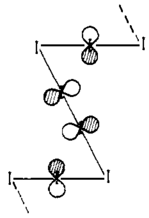

Semiconducting properties

Experimental data related to the PI chains without host are not available. In what follows we compare our theoretical results with indirect experimental information. The existence of a nonzero energy gap can be inferred for the $(I_5^-)_\infty$ systems from the optical spectrum which shows a well-known strong absorption onset around 2 eV for the starch and related nonconducting complexes[3,8b,17b] where the insulating organic host most probably has an absorption onset at higher energies. The well-conducting PI complexes do not provide direct evidences because they strongly absorb in the low-energy (IR) region because of the electronic transitions there. Our prediction of the $E_{gap} \simeq 1.8$ eV for the $(I_3^-)_\infty$ system thus cannot be confronted with experiments on these systems. Nevertheless, the theoretical trend for the gaps $I_2 > I_3^- > (I_5^-)_\infty > (I_3^-)_\infty$ should be verifiable.

The degree of electron (or hole) delocalization should be larger for $(I_3^-)_\infty$ than for $(I_5^-)_\infty$ as follows immediately from the energy band widths. The band width is in the order of 1.5 eV for $(I_3^-)_\infty$, 0.5 eV for linear $(I_5^-)_\infty$, and 0.1 eV for strongly bent $(I_5^-)_\infty$. Thus $(I_5^-)_\infty$ is coming electronically close to narrow band insulators, as typical organic molecular crystals. $(I_3^-)_\infty$ resembles in this respect the polymeric semiconductors, like undoped polyacetylene $(CH)_x$.[29] This can be also seen from the calculated effective mass values given in Table II. It would be, however, more important to compare the mobilities of the charge carriers, μ. The theoretical estimation of the latter is very difficult, owing partly to the great number of possible scattering mechanisms. One important channel, the interaction with acoustic vibrations, can be approximately characterized by the deformation potential[30] $\delta\epsilon$

$$\delta\epsilon = \Delta E/(\delta a/a)$$

where va is a uniform dilation of the lattice constant a and ΔE the corresponding shift of the edge of the energy band. These are then roughly related[30] as $\mu \simeq (\delta\epsilon)^{-2}$. This indicates that, other factors being equal, electron and hole mobilities in $(I_3^-)_\infty$ are expected to be small compared with those in $(CH)_x$. In most of the real PI complexes, disorder effects[31] may dominate the transport properties.

Acknowledgment. This work has been partly supported by the KKA Project of the Hungarian Academy of Sciences.

Registry No. I_3^-, 14900-04-0; I_5^-, 22318-17-8.

---

(29) (a) H. Shirakawa, T. Ito, and S. Ikeda, *Makromol. Chem.*, **179**, 1565 (1978); (b) C. K. Chiang, A. J. Heeger, and A. G. MacDiarmid, *Ber. Bunsenges. Phys. Chem.*, **83**, 407 (1979), and references therein.

(30) (a) W. Shockley, "Electrons and Holes in Semiconductors", Van Nostrand, Princeton, 1950; (b) F. Beleznay, G. Biczó, and J. Ladik, *Acta Phys. Hung.*, **18**, 213 (1963); (c) M. Kertész, J. Koller, and A. Azman, *Chem. Phys.*, **27**, 273 (1978).

(31) See, e.g., G. Güner, *Chem. Scr.* **17**, 207 (1981).

(32) F. H. Herbstein, M. Kaftory, M. Kapon, and W. Saenger, *Z. Kristallogr.*, **154**, 11 (1981).

Chemical Reaction Paths. 8.[1] Stereoisomerization Path for Triphenylphosphine Oxide and Related Molecules: Indirect Observation of the Structure of the Transition State

Erik Bye,[2] W. Bernd Schweizer, and Jack D. Dunitz*

Contribution from the Organic Chemistry Laboratory, Swiss Federal Institute of Technology, ETH-Zentrum, CH-8092 Zürich, Switzerland. *Received February 2, 1982*

Abstract: The conformations of more than 1000 Ph_3PX molecules or molecular fragments have been retrieved from the Cambridge Crystallographic Data Centre Database. Each observed conformation is regarded as a sample point defined by the rotation angles of the three phenyl groups. From the distribution of such sample points conclusions may be drawn about features of the molecular potential energy surface. In particular, we have been able to chart out low-energy stereoisomerization paths for triphenylphosphine oxide (and related molecules) and to discern the approximate structure of the transition state for this stereoisomerization process.

In this paper we apply the structure correlation method[3,4] to map low-energy stereoisomerization paths for molecules of the type Ph_3PX, e.g., triphenylphosphine oxide and related molecules or fragments of molecules, including metal complexes of triphenylphosphine. Such isomerizations involve mainly rotations of the phenyl groups, and hence we shall be interested mainly in the torsion angles around the three Ph–P bonds. Indeed, we shall

---

(1) Part 7. Britton, D.; Dunitz, J. D. *J. Am. Chem. Soc.* **1981**, *103*, 2971–2979.

(2) On leave of absence from University of Oslo in 1977. Address correspondence to Institute of Occupational Health, Box 8149, Oslo 1, Norway.

(3) (a) Bürgi, H. B. *Inorg. Chem.* **1973**, *12*, 2321–2325. (b) Murray-Rust, P.; Bürgi, H. B.; Dunitz, J. D. *J. Am. Chem. Soc.* **1975**, *97*, 921–922.

(4) Dunitz, J. D. "X-Ray Analysis and the Structure of Organic Molecules"; Cornell University Press: Ithaca, NY, 1979; Chapter 7.

0002-7863/82/1504-5893$01.25/0